the Pc dimer initiates dimeric decomposition to the monomeric Pc anion radical species $\{(Pc)Fe^{I}\}^{2-}$.

To facilitate comparisons, the midpoint potentials for the electrode reactions of the known single atom bridged dimers of Pc and TPP are listed in Table I. Interestingly, the electrode reactions of both $[(Pc)Fe]_2O$ and $[(Pc)Fe]_2N$ are anodic of the corresponding reactions of $[(TPP)Fe]_2O$ and $[(TPP)Fe]_2N$, respectively. This follows the trend previously observed for the monomeric complexes that the phthalocyanine ring stabilizes lower oxidation states of iron in phthalocyanine complexes as compared to the corresponding porphyrin complex.[30] Similarly, the midpoint potentials for $[(Pc)Fe]_2O$ are anodic of the corresponding couple for $[(Pc)Fe]_2N$. However, the potential differences decrease as the negative charge on the dimer increases. If one uses the MO diagram put forth for the TPP single atom bridged dimers[31] as a qualitative description of the MO diagram for the Pc single atom bridged dimers, then this trend is in accord with expectations. Also, one would predict that the HOMO for the μ-oxo complex is localized on the two metal atoms and the bridging moiety rather than the ring. Oxidation of the complex would then decrease the electron density about the metal atom. Note, however, that Hoffmann's MO diagram does not account for axial ligation of the Fe atoms by solvent molecules as has been shown to occur for $[(Pc)Fe]_2O$ by Ercolani et al.[14]

Comparison of the potentials for reduction of the isoelectronic dimers, $\{[(Pc)Fe]_2O\}^+$ to $[(Pc)Fe]_2N$, indicates that the μ-nitrido dimer is stabilized by 1300 mV over that of the analogous mixed-valence Fe^{III}–Fe^{IV} μ-oxo complex. This stabilization is significantly less than the value of 2050 mV observed by Kadish et al.[6] for the corresponding TPP dimers in the noncoordinating solvent CH_2Cl_2. This decrease may be a manifestation of the difference in the donor properties of the macrocycles or it may reflect the influence of a coordinating solvent.

Minor and Lever[32] have previously reported the electron-transfer mechanism of $[(Pc)Mn]_2O$ in pyridine. They observed one reversible oxidation at 0.35 V and a multielectron reduction to a monomeric anion radical species, $\{(Pc)Mn^{II}\}^-$, at −0.85 V. Their data is consistent only with an initial electron transfer involving two electrons, producing $\{[(Pc)Mn^{II}]_2O\}^{2-}$. No evidence for a mixed valence Mn^{III}–Mn^{II} species was obtained. This suggests that the potential for addition of the second electron to this complex must be equal to or anodic of the potential for addition of the first electron. For the corresponding Fe dimer described herein, two sequential one-electron reductions are observed, separated by 360 mV. Clearly, addition of electrons to either dimer populates an antibonding orbital, destabilizing the dimeric linkage. A rational explanation for the observed stabilization of the mixed-valence species for the Fe-containing dimer as compared to the Mn-containing dimer awaits the formulation of a MO description that accounts for changes in the identity of the central metal atom in the dimer, the presence of macrocycles with different donor properties, and the presence of nitrogenous bases producing perturbations at the axial positions of the dimer.

Acknowledgment. L.A.B. wishes to acknowledge the Istituto di Teoria e Struttura Elettronica, CNR, Area della Ricerca di Roma (Montelibretti), for a visiting professorship, kind hospitality, and excellent research facilities.

Registry No. $[(Pc)Fe]_2O$, 74353-48-3; $[(Pc)Fe]_2O^+$, 100228-78-2; $[(Pc)Fe]_2O^-$, 100228-80-6; $[(Pc)Fe]_2O^{2-}$, 100228-81-7; (Pc)Fe, 132-16-1; $(Pc)Fe^-$, 38600-22-5; $(Pc)Fe^{2-}$, 38600-23-6; (Pc)Fe(OH), 80602-48-8; $(Pc)Fe(OH)^-$, 100228-82-8; $[(TPP)Fe]_2O$, 12582-61-5; $[(TPP)Fe]_2O^-$, 54578-55-1; $(TPP)Fe^-$, 54547-68-1; (TPP)Fe, 16591-56-3; $(TPP)Fe^+$, 29484-63-7; $[(Pc)Fe]_2O^{2+}$, 100228-79-3; Bu_4NOH, 2052-49-5; $(Pc)Fe(py)_2$, 20219-84-5; pyridine, 110-86-1.

---

(31) Tatsumi, K.; Hoffmann, R. J. *J. Am. Chem. Soc.* **1981**, *103*, 3328–3341.

(32) Minor, P. C.; Lever, A. B. P. *Inorg. Chem.* **1983**, *22*, 826–830.

Contribution from the Chemistry Department,
The Ohio State University, Columbus, Ohio 43210

Multiple-Equilibria Model Describing the Axial Ligand Dependence of the Dioxygen Affinity of an Iron(II) Lacunar Complex. An Approach to the Regulation of Dioxygen Affinity

Kenneth A. Goldsby, Brian D. Beato, and Daryle H. Busch*

Received November 13, 1985

The dioxygen-binding behavior of the iron(II) lacunar complex chloro(3,11-dibenzyl-14,20-dimethyl-2,12-diphenyl-3,11,15,19,22,26-hexaazatricyclo[11.7.7.1^{5,9}]octacosa-1,5,7,9(28),12,14,19,21,26-nonaene-$\kappa^4 N$)iron(II) hexafluorophosphate in 1.5 M 1-methylimidazole/acetonitrile (1.5 M MIM/AN) is described. Although 1-methylimidazole is known *not* to displace chloride as the axial ligand in acetonitrile (even at concentrations as high as 1.5 M), the lacunar iron(II) complex shows a high affinity for dioxygen in 1.5 M MIM/AN, in spite of the known low dioxygen affinity of the chloro complexes. The high dioxygen affinity of this system has been explained in terms of a trans displacement of the axial chloride by dioxygen. The displacement of chloride can occur via two pathways that incorporate two distinct types of equilibria: (1) equilibria involving the coordination of dioxygen and (2) equilibria involving the exchange of axial ligand. The entire process can be described by a multiple-equilibria model comprised of four separate, but mutually related, equilibria. To a first approximation, the functional dependence of dioxygen adduct formation on the concentration of dioxygen is the same as that expected for a single dioxygen equilibrium. For this reason, one may calculate a single effective binding constant that reflects the dioxygen affinity of this mixed-axial-ligand system. As expected from this model, the dioxygen affinity can be suppressed by the addition of excess chloride. The possibility of continuously regulating the dioxygen affinity over wide ranges by manipulating the concentrations of potential axial bases has been demonstrated, and applications are suggested.

Introduction

The dioxygen affinity of synthetic dioxygen carriers is known to be quite dependent upon the nature of the axial base. Basolo recognized that the equilibrium constant for dioxygen adduct formation (K_{O_2}) for a given cobalt Schiff-base complex varied with the axial base according to the $Co^{III/II}$ half-wave potential ($E_{1/2}$).[1] To account for the linear relationship between log K_{O_2} and $E_{1/2}$ for limited ranges of axial bases, the $Co^{III/II}$ half-wave potential

---

(1) (a) Carter, M. J.; Rillema, D. P.; Basolo, F. *J. Am. Chem. Soc.* **1974**, *96*, 392–400. (b) Carter, M. J.; Engelhardt, L. M.; Rillema, D. P.; Basolo, F. *J. Chem. Soc., Chem. Commun.* **1973**, 810–812.

was taken as a direct measure of the electron density on Co^{II}, which, in turn, is a function of the electron-donating ability of the particular axial base. Although less thoroughly explored, the relationship between dioxygen affinities and axial bases for iron dioxygen carriers has been addressed[2,3] with most examples comparing the dioxygen affinity of iron(II) porphyrins axially coordinated to substituted imidazoles and substituted pyridines. It is generally noted that the imidazole complexes have the higher dioxygen affinities; this is consistent with the greater basicity of imidazole over pyridine.

Our own work has involved the reversible binding of dioxygen to cobalt and iron complexes of the lacunar macrobicyclic cyclidene ligands (structure I).[4-6] As observed for the iron porphyrin systems, the K_{O_2} values for the Fe^{II} lacunar dioxygen carriers with 1-methylimidazole as the axial base were higher than those of the analogous pyridine complexes. Moreover, the complexes with aromatic nitrogenous bases gave much higher K_{O_2}'s than did the complexes with chloride as the axial ligand. This result agrees with the known weak donor ability of chloride. In our earlier studies, the low dioxygen affinity of the chloride complexes presented a particular problem since the Fe^{II} lacunar complexes are generally synthesized with chloride tenaciously bound as the axial ligand. Further, the axial Cl^- is not readily displaced in organic solvents, such as acetonitrile, even by the addition of large excesses of 1-methylimidazole or pyridine. In order to achieve high binding constants for dioxygen with the chloro(lacunar)-iron(II) complexes, the ternary solvent 3:1:1 acetone/pyridine/water was employed. In this mixed solvent, the water solvates the Cl^- ion, facilitating its replacement by pyridine, which then becomes the axial base. In this manner, a highly efficient dioxygen carrier is generated.[6]

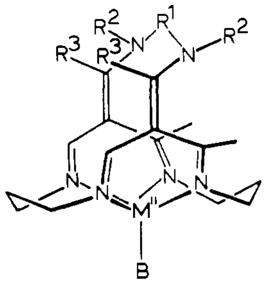

It has been noted that coordination of a sixth ligand (CO[7] or solvent[8]) can act to labilize the axial chloride even in organic solvents such as acetonitrile. We report here the dioxygen affinity of $[Fe\{Ph_2(BzN)_2(m\text{-xyl})[16]cyclidene\}Cl]^+$ (structure I where M is Fe^{II}, R^3 is phenyl, R^2 is benzyl, R^1 is *m*-xylyl (*m*-xyl), and B is chloride) in 1.5 M 1-methylimidazole/acetonitrile, where O_2 itself has been used to labilize the axial chloride, giving the dioxygen adduct with 1-methylimidazole as the axial base. The high dioxygen affinity has been explained in terms of a model incorporating two types of equilibria: (1) equilibria involving the coordination of dioxygen and (2) equilibria involving the exchange of axial ligands. Furthermore, the effective dioxygen affinity based on total iron complex is found to be strongly dependent upon the concentration of free chloride. The net result is a dioxygen carrier in which the overall dioxygen affinity can be *adjusted* continuously by variations in the concentration of chloride ion.

Table I. Dioxygen Binding Constants for the Complexes $[Fe\{Ph_2(BzN)_2(m\text{-xyl})[16]cyclidene\}B]^{n+}$[a] in Acetonitrile

B	solvent[b]	T, K	K_{O_2}, $torr^{-1}$ (σ, $torr^{-1}$)[c]
CH_3CN	1.5 M MIM/AN	273	1.6×10^{-2}[d]
Cl	1.5 M MIM/AN	273	5.3×10^{-3} (6.0×10^{-4})
Cl	neat AN	233	4.0×10^{-3} (1.6×10^{-4})[e]
Cl	neat AN	273	(10^{-5})[f]

[a] B is the axial base coordinated to the (lacunar)iron(II) complex. When B = CH_3CN, n = 2; when B = Cl^-, n = 1. [b] MIM is 1-methylimidazole; AN is acetonitrile. [c] K_{O_2} is the average of K_{O_2} values determined for at least three different wavelengths; σ is the largest standard deviation of the individual K_{O_2} determinations. [d] Reference 6. [e] At all pressures the chloro(lacunar)iron(II) complex was a poor dioxygen carrier; however, good fits for K_{O_2} could be obtained only when the low dioxygen partial pressure data (<100 torr) was omitted. [f] Estimated from thermodynamic parameters; note text and ref 6.

Experimental Section

Materials. Acetonitrile and 1-methylimidazole were dried by recommended procedures[9] and distilled under N_2 before use. The complex chloro(3,11-dibenzyl-14,20-dimethyl-2,12-diphenyl-3,11,15,19,22,26-hexaazatricyclo[11.7.7.1^{5,9}]octacosa-1,5,7,9(28),12,14,19,21,26-nonaene-$\kappa^4 N$)iron(II) hexafluorophosphate was synthesized according to a published procedure[6] and generously provided by Dr. Lyndel Dickerson.

Physical Measurements. Visible spectral data were obtained with a Varian 2300 recording spectrophotometer. Exposure of thermostated solutions of the Fe^{II} lacunar complex to various partial pressures of dioxygen was achieved with a series of calibrated rotometers or flow meters, as previously described.[6]

Dioxygen binding constants were obtained by the method of Stevens[10] using a program written by Naidong Ye of this group. This involves monitoring electronic spectral changes as a function of dioxygen partial pressure at three or four different wavelengths, as previously described.[6] Solutions of the Fe^{II} lacunar complex were degassed with a stream of dioxygen-free N_2 for 500 s, in order to insure that the initial absorbance measurements (A_0) were obtained in the absence of dioxygen. Data consisting of partial pressures of dioxygen and the corresponding ratios of absorbance at a given partial pressure to absorbance at zero partial pressure (A/A_0) were fit to eq 27 by using a grid-search nonlinear least-squares program from Dr. Michael H. Klapper.

Electrochemical measurements were made with a PAR Model 173 potentiostat for potential control and a PAR Model 175 universal programer as a sweep generator for voltammetry measurements. Current vs. potential curves were measured on a Houston Instruments Model 2000 XY recorder. All solutions for electrochemical studies were prepared in a glovebox under an atmosphere of dry dinitrogen. Routine measurements were made in a glovebox at a platinum-disk electrode vs. a Ag/0.1 M $AgNO_3/CH_3CN$ reference electrode. For studies requiring exposure to dioxygen, measurements were carried out in a two-compartment cell joined by a glass frit. One compartment was equipped with a gas inlet and bubbling tube. In the compartment equipped for bubbling, two platinum wires sealed into a ground-glass joint served as the working and auxiliary electrodes. In the other compartment, a silver wire served as a pseudoreference electrode. In these experiments, the ferrocenium/ferrocene couple was employed as an internal reference.[11] All electrochemical measurements were carried out with 0.1 M tetrabutylammonium tetrafluoroborate (TBAT) as the supporting electrolyte.

Results and Discussion

Labilization of Chloride by Dioxygen. The chloride-free analogue of $[Fe\{Ph_2(BzN)_2(m\text{-xyl})[16]cyclidene\}Cl]^+$ has been synthesized in which the Cl^- axial ligand is replaced with a solvent molecule, presumably acetonitrile.[6] This complex, $[Fe\{Ph_2(BzN)_2(m\text{-xyl})[16]cyclidene\}CH_3CN]^{2+}$, displays a moderately high affinity for dioxygen in solvents containing a large excess of some aromatic nitrogenous base. For example, in 1.5 M 1-

---

(2) Traylor, T. G.; Traylor, P. S. *Annu. Rev. Biophys. Bioeng.* **1982**, *11*, 105–127.

(3) Collman, J. P.; Brauman, J. I.; Doxsee, K. M; Sessler, J. L.; Morris, R. M.; Gibson, Q. H. *Inorg. Chem.* **1983**, *22*, 1427–1432.

(4) Stevens, J. C.; Busch, D. H. *J. Am. Chem. Soc.* **1980**, *102*, 3285–3287.

(5) (a) Herron, N.; Busch, D. H. *J. Am. Chem. Soc.* **1981**, *103*, 1236–1237. (b) Herron, N.; Cameron, J. H.; Near, G. L.; Busch, D. H. *J. Am. Chem. Soc.* **1983**, *105*, 298–301.

(6) Herron, N.; Zimmer, L. L.; Grzybowski, J. J.; Olszanski, D. J.; Jackels, S. C.; Callahan, R. W.; Cameron, J. H.; Christoph, G. G.; Busch, D. H. *J. Am. Chem. Soc.* **1983**, *105*, 6585–6596. The K_{O_2} values reported here for 4:1 solvent/MIM were actually measured in 1.5 M MIM/solvent, where the solvent is toluene, acetonitrile, water, methanol, and acetone: Herron, N., personal communication.

(7) Busch, D. H.; Zimmer, L. L.; Grzybowski, J. J.; Olszanski, D. J.; Jackels, S. C.; Callahan, R. W.; Christoph, G. G. *Proc. Natl. Acad. Sci. U.S.A.* **1981**, *78*, 5919–5923.

(8) Herron, N.; Schammel, W. P.; Jackels, S. C.; Grzybowski, J. J.; Zimmer, L. L.; Busch, D. H. *Inorg. Chem.* **1983**, *22*, 1433–1440.

(9) Vogel, A. I. *A Textbook of Practical Organic Chemistry*, 3rd ed.; Wiley: New York, 1966; p 163–179.

(10) Stevens, J. C. Ph.D. Dissertation, The Ohio State University, 1979.

(11) Gagné, R. R.; Kovel, C. A.; Lisensky, G. C. *Inorg. Chem.* **1980**, *19*, 2855–2857.

methylimidazole/acetonitrile (1.5 M MIM/AN), K_{O_2} was determined to be 0.016 torr^{-1} at 273 K.[6] Under these same conditions (1.5 M MIM/AN), the chloride complex gives a K_{O_2} of 0.005 torr^{-1}. Although K_{O_2} is a factor of 3 lower than that observed for the CH_3CN analogue, the dioxygen affinity is still surprisingly high given the high binding constant of chloride for the iron lacunar complexes in acetonitrile ($K = 2 \times 10^5$ M^{-1})[7] and the known low dioxygen affinities of the chloro(lacunar)iron(II) complexes.[6]

In order to verify the low dioxygen affinity of the chloro complex, the K_{O_2} of [Fe{Ph$_2$(BzN)$_2$(*m*-xyl)[16]cyclidene}Cl]$^+$ was determined in acetonitrile in the absence of added base. As expected, the binding constant was too low to be measured at 273 K or even 253 K; however, at 233 K an upper limit of 4×10^{-3} torr^{-1} could be estimated. Previous work on the iron(II) lacunar complexes in 3:1:1 acetone/pyridine/water has yielded thermodynamic parameters for dioxygen binding from van't Hoff plots,[6] and on the basis of this work K_{O_2} for the chloro complex in neat acetonitrile at 273 K would be expected to be about 10^{-5} torr^{-1}. The dioxygen binding constants for the various iron(II) lacunar systems described above are summarized in Table I.

Although the high binding constant observed for the chloro(lacunar)iron(II) complex dissolved in 1.5 M MIM/AN is *not* consistent with the presence of chloride bound as the axial ligand, it is known from the visible spectra, conductivity, and electrochemistry of solutions of the chloro(lacunar)iron(II) complexes in acetonitrile containing large excesses of 1-methylimidazole that the chloride axial ligand is not displaced.[6] The resolution of this apparent paradox is achieved by recognizing that dioxygen must somehow labilize the axial chloride, giving the dioxygen adduct with 1-methylimidazole as the axial base. The labilization of chloride has been noted in the formation of CO adducts with these same chloro(lacunar)iron(II) complexes (eq 1).[7] Furthermore,

$$[Fe(L)Cl]^+ + CO + B \rightarrow [Fe(L)B(CO)]^{2+} + Cl^- \qquad (1)$$

dimeric complexes based on the iron(II) cyclidene unit do not show the same high binding constant with chloride as do the monomeric lacunar complexes; this presumably results from the ease with which the dinuclear species become six-coordinate in solution, resulting in trans labilization of the axial chloride.[8] It is reasonable that dioxygen would have the same effect on axial chloride so that coordination of dioxygen at the sixth coordination site labilizes the trans chloride, enabling 1-methylimidazole to bind at that position (eq 2 and 3). Alternatively, a small but finite

$$[Fe(L)Cl]^+ + O_2 \rightleftharpoons [Fe(L)Cl(O_2)]^+ \qquad (2)$$

$$[Fe(L)Cl(O_2)]^+ + B \rightleftharpoons [Fe(L)B(O_2)]^{2+} + Cl^- \qquad (3)$$

$$B = \text{1-methylimidazole}$$

amount of the complex with 1-methylimidazole as the axial base may exist in solution and, given the much higher dioxygen affinity of the 1-methylimidazole complex, the equilibrium would be driven by dioxygen toward the 1-methylimidazole adduct (eq 4 and 5).

$$[Fe(L)Cl]^+ + B \rightleftharpoons [Fe(L)B]^{2+} + Cl^- \qquad (4)$$

$$[Fe(L)B]^{2+} + O_2 \rightleftharpoons [Fe(L)B(O_2)]^{2+} \qquad (5)$$

In the preceding discussion, we have represented the dissociation of chloride as an equilibrium process. It might be argued that the dioxygen-binding behavior of the chloro(lacunar)iron(II) complexes could be explained in terms of a kinetically slow dissociation of chloride which is facilitated by the trans labilization with dioxygen. To address this point, cyclic voltammograms were obtained of the complex [Fe{Ph$_2$(BzN)$_2$(*m*-xyl)[16]cyclidene}Cl]$^+$ in 1.5 M MIM/AN at 253 K. The initial voltammogram showed an irreversible[12] oxidation at −0.19 V vs. the ferrocenium/ferrocene couple, corresponding to the Fe–Cl species. After bubbling O_2 through the solution for several minutes, the subsequent voltammogram gave no indication of the Fe–Cl species.[14] The solution was then purged with N_2 for approximately 10 min, after which the Fe–Cl oxidation was observed in the voltammogram at essentially the same intensity. This was repeated through several cycles. These results suggest that the dissociation of chloride in this system can be reasonably represented as an equilibrium-controlled process.

Scheme I

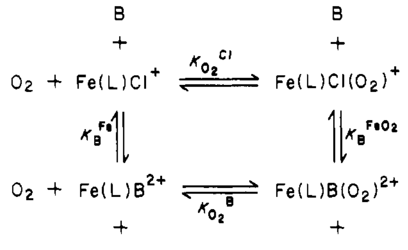

Regardless of which mechanism dominates (eq 2 and 3 or eq 4 and 5), the dioxygen affinity of the iron(II) lacunar system is governed by two distinct types of equilibria: (1) equilibria between the oxygenated and unoxygenated complexes, eq 2 and 5, and (2) equilibrium between the chloride and 1-methylimidazole complexes, eq 3 and 4. In the next section we will consider the implications of this multiple-equilibria model.

Multiple-Equilibria Model. For the simple system consisting of the equilibrium between an oxygenated and unoxygenated complex (eq 6), the dioxygen binding constant is given by eq 7.

$$Fe(L) + O_2 \overset{K_{O_2}}{\rightleftharpoons} Fe(L)(O_2) \qquad (6)$$

$$K_{O_2} = \frac{[Fe(L)(O_2)]}{[Fe(L)][O_2]} \qquad (7)$$

Since Fe(L) and Fe(L)(O$_2$) are the species in this system that absorb visible light, the overall absorbance at a particular wavelength will be given by eq 8,[15] where ϵ_{Fe} and ϵ_{FeO_2} are the

$$A = \epsilon_{Fe}[Fe(L)] + \epsilon_{FeO_2}[Fe(L)(O_2)] \qquad (8)$$

molar extinction coefficients of the unoxygenated and oxygenated species, respectively. Substituting eq 7 and an equation for material balance (eq 9) into eq 8 gives an expression for total absorbance at a particular wavelength as a function of the concentration of dioxygen (eq 10).

$$[Fe_T] = [Fe(L)] + [Fe(L)(O_2)] \qquad (9)$$

$$A = \left[\frac{\epsilon_{Fe} + \epsilon_{FeO_2}K_{O_2}[O_2]}{1 + K_{O_2}[O_2]}\right][Fe_T] \qquad (10)$$

Given the low concentration of iron complex used in these experiments (typically 10^{-3}–10^{-4} M) and the inherent difficulties in obtaining accurate weight measurements in an inert-atmosphere box, it is convenient to use the initial absorbance of the iron complex *before* exposure to dioxygen (A_0) as a measurement of concentration;[16] note eq 11, where [Fe$_T$] is the total concentration

$$A_0 = \epsilon_{Fe}[Fe_T] \qquad (11)$$

---

(12) At room temperature, the Fe$^{III/II}$ couple is reversible; at 253 K the couple becomes irreversible, possibly due to the formation of oxo-bridged dimer as a result of the deprotonation of residual water in the solvent by the 1-methylimidazole.[13]

(13) Goldsby, K. A., work in progress.

(14) Redox processes assignable to an oxygenated species were not identified, possibly due to the limits of the potential range available in an O_2-saturated solution of 1.5 M MIM/AN.

(15) In this work, all spectroscopic measurements were carried out in cells with a path length of 1 cm, so in this and subsequent Beer's law expressions (eq 11, 19, 25), the path length has been omitted.

(16) For the spectral region employed in this study (500–560 nm), the chloro(lacunar)iron(II) complex exhibits a sufficiently strong absorption to allow accurate determinations of relative concentration.

of iron complex. Substituting eq 11 into eq 10 gives an expression for A/A_0 as a function of the concentration of dioxygen (eq 12).

$$\frac{A}{A_0} = \frac{1 + (\epsilon_{FeO_2}/\epsilon_{Fe})K_{O_2}[O_2]}{1 + K_{O_2}[O_2]} \qquad (12)$$

This picture is made considerably more complicated by the introduction of an axial-base equilibrium. In Scheme I, eq 2–5 are combined to illustrate the interrelationship between the four equilibria. Expressions for the individual equilibrium constants are given in eq 13–16. An important point to note early in this discussion is that the four equilibria are *not* mutually independent. It can be easily shown that the four equilibrium constants are related by eq 17. This suggests that any perturbation of the system, such as the addition of excess axial ligand, will effect the entire distribution of species. We will return to this point later in the discussion.

$$K_{O_2}{}^{Cl} = \frac{[Fe(L)Cl(O_2)^+]}{[Fe(L)Cl^+][O_2]} \qquad (13)$$

$$K_{O_2}{}^{B} = \frac{[Fe(L)B(O_2)^{2+}]}{[Fe(L)B^{2+}][O_2]} \qquad (14)$$

$$K_B{}^{Fe} = \frac{[Fe(L)B^{2+}][Cl^-]}{[Fe(L)Cl^+][B]} \qquad (15)$$

$$K_B{}^{FeO_2} = \frac{[Fe(L)B(O_2)^{2+}][Cl^-]}{[Fe(L)Cl(O_2)^+][B]} \qquad (16)$$

$$\frac{K_B{}^{Fe}K_{O_2}{}^{B}}{K_B{}^{FeO_2}K_{O_2}{}^{Cl}} = 1 \qquad (17)$$

As with the simple dioxygen model presented earlier, we can write expressions for material balance (eq 18) and total absorbance (eq 19) in terms of the concentrations and extinction coefficients of the individual species. As before, substituting any three of eq 13–16 and eq 18 into eq 19 yields the following expression for absorbance as a function of the concentrations of dioxygen, chloride, and base:

$$[Fe_T] = [Fe(L)Cl^+] + [Fe(L)B^{2+}] + [Fe(L)Cl(O_2)^+] + [Fe(L)B(O_2)^{2+}] \qquad (18)$$

$$A = \epsilon_{FeCl}[Fe(L)Cl^+] + \epsilon_{FeB}[Fe(L)B^{2+}] + \epsilon_{FeClO_2}[Fe(L)Cl(O_2)^+] + \epsilon_{FeBO_2}[Fe(L)B(O_2)^{2+}] \qquad (19)$$

$$A = \left[\frac{W + X[O_2]}{Y + Z[O_2]}\right][Fe_T] \qquad (20)$$

where

$$W = \epsilon_{FeCl}K_{O_2}{}^{B}[Cl^-] + \epsilon_{FeB}K_{O_2}{}^{Cl}K_B{}^{FeO_2}[B] \qquad (21)$$

$$X = \epsilon_{FeClO_2}K_{O_2}{}^{Cl}K_{O_2}{}^{B}[Cl^-] + \epsilon_{FeBO_2}K_{O_2}{}^{Cl}K_{O_2}{}^{B}K_B{}^{FeO_2}[B] \qquad (22)$$

$$Y = K_{O_2}{}^{B}[Cl^-] + K_{O_2}{}^{Cl}K_B{}^{FeO_2}[B] \qquad (23)$$

$$Z = K_{O_2}{}^{Cl}K_{O_2}{}^{B}[Cl^-] + K_{O_2}{}^{Cl}K_{O_2}{}^{B}K_B{}^{FeO_2}[B] \qquad (24)$$

It is interesting to note that the individual terms in the numerator and denominator of eq 20 are identical except that the terms in the numerator are weighed by the extinction coefficients of the absorbing species.

As before, it is desirable to use the initial absorbance before the addition of dioxygen as a measure of the total iron concentration. For the model system described above, A_0 is given by eq 25. Combining expressions for Beer's law, material balance, and equilibrium in a treatment similar to that employed for the single dioxygen equilbrium case (eq 6–12), an expression for A_0 is obtained as given in eq 26. Substitution of eq 26 into eq 20 and rearranging terms give

$$A_0 = \epsilon_{FeCl}[Fe(L)Cl^+] + \epsilon_{FeB}[Fe(L)B^{2+}] \qquad (25)$$

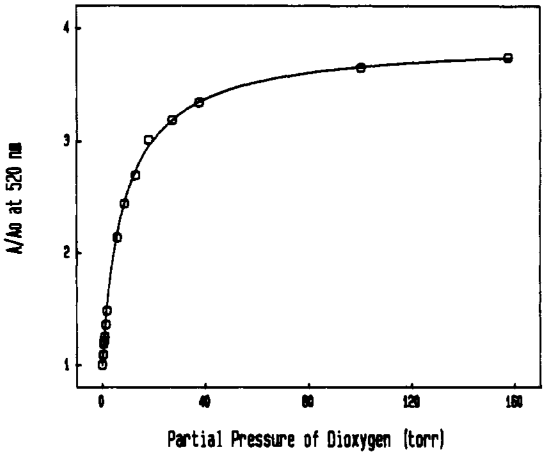

Figure 1. A/A_0 at 520 nm vs. the partial pressure of dioxygen in torr for [Fe{$Ph_2(BzN)_2$(*m*-xyl)[16]cyclidene}Cl]$^+$ in 1.5 M 1-methylimidazole/acetonitrile at 253 K. The solid line corresponds to the nonlinear least-squares fit of the data to eq 27.

$$A_0 = \left[\frac{\epsilon_{FeCl}[Cl^-] + \epsilon_{FeB}K_B{}^{Fe}[B]}{[Cl^-] + K_B{}^{Fe}[B]}\right][Fe_T] \qquad (26)$$

$$\frac{A}{A_0} = \frac{1 + U[O_2]}{1 + V[O_2]} \qquad (27)$$

where

$$U = [\epsilon_{FeClO_2}K_{O_2}{}^{Cl}K_{O_2}{}^{B}[Cl^-] + \epsilon_{FeBO_2}K_{O_2}{}^{Cl}K_{O_2}{}^{B}K_B{}^{FeO_2}[B]][[Cl^-] + K_B{}^{Fe}[B]]/\{[\epsilon_{FeCl}[Cl^-] + \epsilon_{FeB}K_B{}^{Fe}[B]][K_{O_2}{}^{B}[Cl^-] + K_{O_2}{}^{Cl}K_B{}^{FeO_2}[B]]\} \qquad (28)$$

$$V = [K_{O_2}{}^{Cl}K_{O_2}{}^{B}[Cl^-] + K_{O_2}{}^{Cl}K_{O_2}{}^{B}K_B{}^{FeO_2}[B]]/[K_{O_2}{}^{B}[Cl^-] + K_{O_2}{}^{Cl}K_B{}^{FeO_2}[B]] \qquad (29)$$

A few points are worth noting. In the extreme case where $\epsilon_{FeCl} = \epsilon_{FeB} = \epsilon_{FeClO_2} = \epsilon_{FeBO_2}$, then $A/A_0 = 1$ as required and there is no change in absorbance with changing dioxygen pressure. Also, as $[Cl^-] \rightarrow O$, eq 27 simplifies to eq 12, which is a natural consequence of turning off the axial-base equilibria, giving the simple dioxygen equilibrium model.

The dioxygen-binding behavior of [Fe{$Ph_2(BxN)_2$(*m*-xyl)[16]cyclidene}Cl]$^+$ in 1.5 M MIM/AN at 253 K is fit quite well by eq 27, as shown in Figure 1. The values obtained for *U* and *V* are 0.450 and 0.116, respectively. In terms of its functional dependence on $[O_2]$, eq 27 has the same form as the comparable expression for the single dioxygen equilibrium model (eq 12). Therefore, it is not surprising that one is able to fit the absorbance vs. partial pressure of dioxygen data for [Fe{$Ph_2(BzN)_2$(*m*-xyl)[16]cyclidene}Cl]$^+$ in 1.5 M MIM/AN to the single dioxygen equilibrium model and hence a single K_{O_2}. The data presented in Figure 1 for the Fe–Cl complex in 1.5 M MIM/AN gives an apparent K_{O_2} value of 0.12 torr^{-1}.[17] However, as the discussion above indicates, the value obtained from the fit is *not* an actual equilibrium constant but rather a conglomeration of concentrations and equilibrium constants combined into a single parameter.

---

(17) Strictly speaking, the expressions for K_{O_2} have been defined in terms of the concentration of dioxygen ($[O_2]$); however, in the absence of solubility data for dioxygen in 1.5 M MIM/AN, we have employed partial pressures of dioxygen (P_{O_2}) as a measure of concentration (i.e., $K_{O_2} = [Fe(L)(O_2)]/([Fe(L)]P_{O_2})$). As a result of this, the K_{O_2} values are reported in units of torr^{-1}.

Table II. Functional Parameters and Effective Dioxygen Binding Constants for $[Fe\{Ph_2(BzN)_2(m\text{-xyl})[16]cyclidene\}Cl]^+$ in 1.5 M MIM/AN at 253 K

salt concn[a]	U (σ)[b]	V (σ)[b]	$K_{O_2}^{eff}$, torr^{-1}, (σ, torr^{-1})[c]
0.1 M PF_6^-	4.7×10^{-1} (1.2×10^{-2})	1.64×10^{-1} (5.0×10^{-3})	2.3×10^{-1} (3.2×10^{-2})
0.05 M PF_6^-/0.05 M Cl^-	3.64×10^{-2} (1.9×10^{-4})	1.76×10^{-2} (1.1×10^{-4})	1.7×10^{-2} (1.9×10^{-3})
0.1 M Cl^-	2.28×10^{-2} (1.5×10^{-4})	1.22×10^{-2} (9.2×10^{-5})	1.0×10^{-2} (6.4×10^{-4})[d]

[a] In all cases, the cation is Et_4N^+. [b] Obtained from nonlinear least-squares fit of the spectral data at 520 nm to eq 27; σ is the standard deviation for the fit. [c] $K_{O_2}^{eff}$ is the average of K_{O_2} values determined for at least three different wavelengths; σ is the largest standard deviation of the individual K_{O_2} determinations. [d] Overall spectral changes were too small to allow K_{O_2} to be determined at multiple wavelengths; $K_{O_2}^{eff}$ reported here is for the data at 520 nm.

Instead, the apparent K_{O_2} obtained from applying the single-equilibrium model to the multiple-equilibria system serves as a measure of the innate ability of the system to bind dioxygen and hence is an effective dioxygen binding constant ($K_{O_2}^{eff}$).

In the above discussion, we have tacitly assumed that the concentrations of Cl^- and B are independent of dioxygen concentrations. Strictly speaking, this is not true. In the next section we consider the explicit relationships between axial-ligand concentrations and dioxygen affinity.

Effect of Added Chloride on Dioxygen Affinity. Let us begin with the case where no Cl^- is added to the solution of the chloro(lacunar)iron(II) complex. For the system consisting of a dilute solution of $[Fe\{Ph_2(BzN)_2(m\text{-xyl})[16]cyclidene\}Cl]^+$ in 1.5 M MIM/AN, the concentration of 1-methylimidazole remains essentially constant at 1.5 M, independent of the concentration of dioxygen. In contrast, the concentration of free Cl^- is quite dependent on the concentration of dioxygen, since Cl^- is liberated by the chloro(lacunar)iron(II) complex in route to the 1-methylimidazole–dioxygen adduct. An expression for the concentration of free Cl^- in terms of the concentrations of the different iron species in solution is given in eq 30. Substituting the appropriate equations for material balance and equilibrium constants into eq 30 gives a quadratic equation, which may be solved to yield the following expression for $[Cl^-]$:

$$[Cl^-] = [Fe_T] - [Fe(L)Cl^+] - [Fe(L)Cl(O_2)^+] \quad (30)$$

$$[Cl^-] = \frac{(S^2 + 4K_{O_2}^{B}[Fe_T]S)^{1/2} - S}{2K_{O_2}^{B}} \quad (31)$$

where

$$S = K_{O_2}^{Cl}K_B^{FeO_2}[B]\left[\frac{1 + K_{O_2}^{B}[O_2]}{1 + K_{O_2}^{Cl}[O_2]}\right] \quad (32)$$

Although eq 31 is quite complicated, it does provide a few insights. The $[O_2]$ dependence of $[Cl^-]$ appears as the ratio $(1 + K_{O_2}^{B}[O_2])/(1 + K_{O_2}^{Cl}[O_2])$. It follows that the concentration of chloride will be independent of $[O_2]$ at (1) very low concentrations of dioxygen, corresponding to the situation where there is no dioxygen adduct and $[Cl^-]$ is determined by K_B^{Fe} (eq 4), and (2) very high concentration of dioxygen, corresponding to the situation where all of the iron complex exists as a dioxygen adduct and $[Cl^-]$ is determined by $K_B^{FeO_2}$ (eq 3). For our system, this translates to $[Cl^-] \rightarrow 0$ as $[O_2] \rightarrow 0$ and $[Cl^-] \rightarrow [Fe_T]$ as $[O_2] \rightarrow \infty$. Between these two extremes, $[Cl^-]$ will be a function of $[O_2]$, as indicated above. The good fit to eq 27 in Figure 1—in spite of the $[O_2]$ dependence of $[Cl^-]$—suggests that in the absence of added chloride, U and V (eq 28 and 29) must be dominated by the [B] terms.

For the system presented here, where $K_{O_2}^{B} \gg K_{O_2}^{Cl}$, the dissociation of chloride must occur in order to produce the high binding constants observed. Therefore, independent of the mechanism of the displacement of chloride by dioxygen (eq 2 and 3 or eq 4 and 5), the addition of excess chloride to the system should suppress the dissociation of chloride and hence reduce the dioxygen affinity. The effect of added chloride on the dioxygen-binding behavior of $[Fe\{Ph_2(BzN)_2(m\text{-xyl})[16]cyclidene\}Cl]^+$ in 1.5 M MIM/AN is shown graphically in Figures 2 and 3 and summarized in Table II.

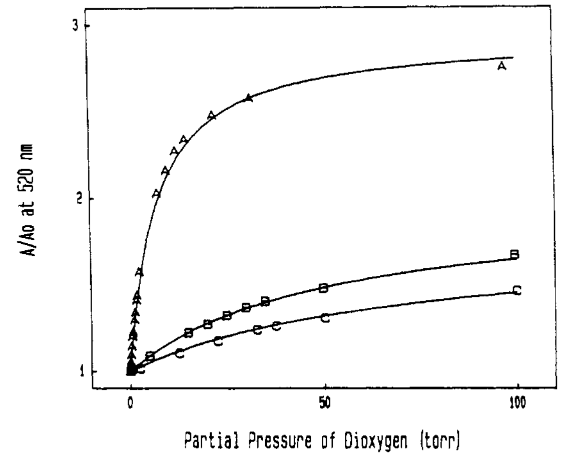

Figure 2. A/A_0 at 520 nm vs. the partial pressure of dioxygen in torr for $[Fe\{Ph_2(BzN)_2(m\text{-xyl})[16]cyclidene\}Cl]^+$ in 1.5 M 1-methylimidazole/acetonitile at 253 K in the presence of (A) 0.1 M $Et_4N^+PF_6^-$, (B) 0.05 M $Et_4N^+PF_6^-$ plus 0.05 M $Et_4N^+Cl^-$, and (C) 0.1 M $Et_4N^+Cl^-$. The solid lines correspond to the nonlinear least-squares fit of the data to eq 27. The fit includes data at higher pressure not shown in the figure.

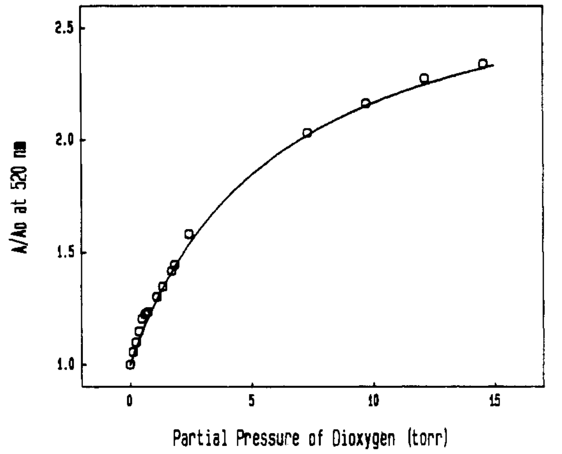

Figure 3. Graph of part A from Figure 2 expanded in the region of 0–15 torr.

In the experiment the concentration of added salt is held constant at 0.1 M. In the presence of 0.1 M $Et_4N^+PF_6^-$ (Figure 3 and graph A of Figure 2), the effective dioxygen binding constant is larger than that observed in the absence of added salt, i.e. 0.23 torr^{-1} vs. 0.12 torr^{-1}. It is well established that increased polarity of the medium enhances dioxygen affinity. Here, increasing the ionic strength should also result in an increased ability of the organic medium to solvate Cl^- and hence promote the replacement of chloride and the formation of the 1-methylimidazole–dioxygen adduct. In contrast, the addition of $Et_4N^+Cl^-$ (Figure 2b,c) results in a sharp reduction in the dioxygen affinity of the system, consistent with a suppression of chloride replacement. In each case the dioxygen-binding behavior can be fit quite nicely to eq 27. In the experiments involving added chloride, U and V are no longer dominated by the [B] terms. Instead, $[Cl^-]$ is now truly independent of $[O_2]$ since [added Cl^-] $\gg$ $[Fe_T]$. The values obtained for U and V, as well as the effective dioxygen binding constants, are given in Table II.

So, it is apparent that the dioxygen affinity of the system formed from the dissolution of $[Fe\{Ph_2(BzN)_2(m\text{-xyl})[16]\text{cyclidene}\}Cl]^+$ in 1.5 M MIM/AN can be adjusted by the addition of chloride. In principle, it should be possible to regulate the dioxygen affinity of a wide variety of synthetic dioxygen carriers by controlling the relative concentrations of two, three, or even more potential axial bases. The ability to precisely regulate dioxygen affinity might eventually have application in the design of O_2 separation and storage devices.[18]

Acknowledgment. The support of the National Science Foundation is gratefully acknowledged. We also thank Dr. Lyndel Dickerson for the development and use of the computer graphics software and for providing the iron(II) complex used in this study.

Registry No. $[Fe\{Ph_2(BzN)_2(m\text{-xyl})[16]\text{cyclidene}\}Cl]PF_6$, 102286-59-9; Cl^-, 16887-00-6.

---

(18) (a) Stewart, R. F.; Estep, P. A.; Sebastian, J. J. S. *Inf. Circ.—U.S., Bur. Mines* **1959**, *No. 7906*. (b) Adduci, A. J. *Abstracts of Papers*, 170th National Meeting of the American Chemical Society, Chicago, IL; American Chemical Society: Washington, DC, 1975. (c) Burke, D. P. *Chem. Week* **1980**, *127*(2), 18.

Contribution from the Department of Chemistry and Biochemistry, Texas Tech University, Lubbock, Texas 79409, and Department of Chemistry, State University of New York at Albany, Albany, New York 12222

Kinetic Stability of the Cysteine Adduct with [Tris(2-(2-pyridyl)ethyl)amine]copper(II)

Haesun Kang Baek,[†] Kenneth D. Karlin,[‡] and Robert A. Holwerda*[†]

Received December 9, 1985

A kinetic study of cysteine (cys-SH) oxidation by [tris(2-(2-pyridyl)ethyl)amine]copper(II) ($Cu(tepa)^{2+}$) has been performed with the aim of documenting the influence of thermodynamic driving force on the Cu^{II}–S redox decay rate. By comparison with the analogous complex in which only one methylene group separates the apical nitrogen atom from the pendant pyridyl units ($Cu(tmpa)^{2+}$), the $Cu(tepa)^{2+/+}$ reduction potential (+315 mV vs. NHE, 25 °C, pH 6, I = 0.1 M (MES)) is more positive by 0.46 V. With excess $Cu(tepa)^{2+}$ present, first-order kinetic traces (pH 4.67–12.50) were observed upon following $Cu(tepa)^+$ formation at 340 nm. The rate–pH profiles of cysteine oxidations by $Cu(tepa)^{2+}$ and $Cu(tmpa)^{2+}$ are superficially similar, exhibiting maxima between pH 8 and 9, but electron transfer within (tepa)Cu^{II}-S-cys is faster by 1–2 orders of magnitude in the low- to intermediate-pH range. As is the case for $Cu(tmpa)^{2+}$, the pH dependence of the (tepa)Cu^{II}-S-cys electron transfer rate may be quantitatively understood in terms of three reactant species (I, II, and III; respective rate constants k_1 = 0.65 s^{-1}, k_2 = 1.2 × 10^2 s^{-1}, k_3 = 3.5 × 10^{-2} s^{-1}) related through successive ionization equilibria (pK_{a1} = 8.9, pK_{a2} = 7.6) (25.0 °C, I = 0.1 M ($NaNO_3$)). Respective redox reactivity ratios (tepa rate constant/tmpa rate constant) of intermediates I, II, and III are ≥6.5 × 10^2, 6.0 × 10, and 9 × 10^{-1}, demonstrating that only I and II are affected appreciably by the increase in oxidizing strength from (tmpa)Cu^{II} to (tepa)Cu^{II}. These ratios imply that electron transfer is rate-determining in the decomposition of intermediates I and II. Insensitivity of k_3 to the oxidizing strength of the Cu(II) center suggests that the (tmpa/tepa)Cu^{II}–S,N-cys activation barrier primarily reflects retarded Cu^{II}–S bond stretching leading to reductive elimination of a thiyl radical.

Introduction

Elegant synthetic approaches coupled with careful spectroscopic analyses have led to significant recent advances in the modeling of blue copper protein electronic structure.[1,2] Most copper(II) complexes of biologically important mercapto amino acids are observable only as transients in aqueous solution, however, such that kinetic studies of formation and decay reactions constitute a vital aspect of their characterization.[3] Indeed, not only have such reactivity studies elucidated the diverse redox decay pathways available to Cu^{II}–SR species, but they also represent, in many cases, the only source of thermodynamic parameters relating to copper(II) complexation by mercaptide sulfur.[3–6]

Structural systematics and related trends in physical properties of Cu(I) and Cu(II) in the low-symmetry N_4 and N_2S_2 coordination environments imposed by tripod ligands have been fully developed by Karlin, Zubieta, and co-workers.[7] S-bonded adducts of mercapto amino acids with the trigonal-bipyramidal[8] [tris(2-pyridylmethyl)amine]copper(II) ion, $Cu(tmpa)^{2+}$, were found to exhibit a remarkable degree of kinetic stability in studies of rate dependences on pH, mercaptan structure, and reductant to oxidant concentration ratio.[3,6] In order to document the influence of thermodynamic driving force on the Cu^{II}–SR redox decay rate, a study of cysteine oxidation by [tris(2-(2-pyridyl)ethyl)amine]copper(II) ($Cu(tepa)^{2+}$) is reported here.

Although the tetradentate tmpa and tepa ligands offer identical N_4 donor atoms, the coordination geometries and associated physical properties of their cupric complexes are markedly different.[8] Thus, the structure of $[Cu(tmpa)Cl]^+$ is essentially trigonal bipyramidal with nearly equivalent Cu^{II}–N bond lengths and related bond angles, while $[Cu(tepa)Cl]^+$ exhibits a square-pyramidal geometry in which the bridgehead amine nitrogen atom occupies a basal position trans to the chloride ligand.[7,8] For our purposes, the most significant impact of the additional methylene group in the tepa tripodal arms is a +0.56-V shift in Cu(II,I) reduction potential (Cl^- complexes in DMF, 0.11 M $N(n\text{-}C_4H_9)_4PF_6$).[8] To the extent that electron transfer from coordinated thiolate sulfur to copper(II) is rate-determining, such an increase in oxidizing strength should be reflected in an enhanced redox decay rate. Since Cu^{II}–S bond stretching is equally important in a reductive elimination process,[3,6] comparative insensitivity of the Cu^{II}–SR redox decay rate to thermodynamic driving force would indicate that the activation barrier is derived mainly from bond-breaking or other structural rearrangement.

Experimental Section

Materials. Reagent grade L-cysteine (cys-SH), 2-morpholinoethanesulfonic acid (MES), and 2-(bis(2-hydroxyethyl)amino)ethanesulfonic acid (BES) were used as supplied by Sigma. (Hydroxyethyl)ferrocene (Strem) was purified by vacuum sublimation. Tris(2-(2-pyridyl)ethyl)amine was prepared and characterized as described by Karlin et al.[8] $[Cu(tepa)(H_2O)](ClO_4)_2\cdot H_2O$ was synthesized through the addition of

---

[†] Texas Tech University.

[‡] State University of New York at Albany.

(1) *Copper Coordination Chemistry*; Karlin, K. D., Zubieta, J., Eds.; Adenine: Guilderland, NY, 1983.

(2) Schugar, H. J., submitted for publication.

(3) Baek, H. K.; Holwerda, R. A. *Inorg. Chem.* **1983**, *22*, 3452.

(4) Stevens, G. D.; Holwerda, R. A. *Inorg. Chem.* **1984**, *23*, 2777.

(5) Anderson, C. A.; Holwerda, R. A. *J. Inorg. Biochem.* **1985**, *23*, 29.

(6) Baek, H. K.; Cooper, R. L.; Holwerda, R. A. *Inorg. Chem.* **1985**, *24*, 1077.

(7) Zubieta, J.; Karlin, K. D.; Hayes, J. C. In ref 1, p 97.

(8) Karlin, K. D.; Hayes, J. C.; Juen, S.; Hutchinson, J. P.; Zubieta, J. *Inorg. Chem.* **1982**, *21*, 4106.

(9) Karlin, K. D.; Hayes, J. C.; Hutchinson, J. P.; Hyde, J. R.; Zubieta, J. *Inorg. Chim. Acta* **1982**, *64*, L219.

0020-1669/86/1325-2347$01.50/0 © 1986 American Chemical Society